

Evolution of the color dipole cross section

G.R.Boroun*

Physics Department, Razi University, Kermanshah 67149, Iran
(Dated: July 4, 2024)

Using Laplace transform techniques, we describe the evolution of the color dipole cross section, at the leading-order and next-to-leading order approximations, from the Bartels-Golec-Biernat-Kowalski model in a kinematical region of low values of the Bjorken variable x and a wide range of transverse dipole size r . This evolution method shows that the saturation scale and geometric scaling are retained. We derived analytical results for the integrated and unintegrated color dipole gluon distribution functions and compared them with the CJ15 parametrization group and the unintegrated color dipole gluon distribution models respectively. The Sudakov form factor into the evolution of the unintegrated color dipole gluon distribution is incorporated and the results are considered at small and large values of k_t^2 .

1. Introduction

In the color dipole model (CDM), the virtual photon γ^* exchanged between the electron and proton currents with virtuality Q^2 , split into a quark-antiquark pair (a dipole) which then interacts with the target proton via gluon exchanges [1]. The quark and antiquark in this dipole carry a fraction z and $1 - z$ of the photon longitudinal momentum respectively. The transverse size between the quark and antiquark is given by the vector \mathbf{r} . The interaction of small-sized color dipoles with nucleons is governed by perturbative QCD (pQCD) and also the basic dipole-factorization holds at large dipole sizes [2]. The total γ^*p cross section is given by

$$\sigma_{L,T}^{\gamma^*p}(x, Q^2) = \sum_f \int d^2\mathbf{r} \int_0^1 dz |\Psi_{L,T}(\mathbf{r}, z; Q^2)|^2 \sigma_{\text{dip}}(x, \mathbf{r}), \quad (1)$$

where the sum over quark flavours f is performed. Here x is the Bjorken scaling and $\Psi_{L,T}(\mathbf{r}, z; Q^2)$ are the appropriate spin averaged light-cone wave functions of the photon, which give the probability for the occurrence of a $(q\bar{q})$ fluctuation of transverse size with respect to the photon polarization [3]. The photon wave function depends on the mass of the quarks in the $q\bar{q}$ dipole, therefore contributions depend on the mass of the quarks by modifying the Bjorken variable x in the dipole cross section as $x \rightarrow \tilde{x}_f \equiv x(1 + 4m_c^2/Q^2)$ with the number of active flavor $n_f = 4$ where m_c is the mass of the quark of charm (with $m_c = 1.4$ GeV).

The dipole cross-section, $\sigma_{\text{dip}}(x, r)$, which related to the imaginary part of the $(q\bar{q})p$ forward scattering amplitude, in the Golec-Biernat-Wusthof (GBW) model [4] is defined by the following form

$$\sigma_{\text{dip}}(x, \mathbf{r}) = \sigma_0 \left\{ 1 - \exp \left(-r^2 Q_{\text{sat}}^2(x)/4 \right) \right\}, \quad (2)$$

where $Q_{\text{sat}}(x)$ plays the role of the saturation by the form $Q_{\text{sat}}^2(x) = Q_0^2(x_0/x)^\lambda$ ($Q_0^2 = 1$ GeV²) and it becomes a function of a single variable rQ_s (for all values of r and x) as has a property of geometric scaling [5] by the following form

$$\sigma_{\text{dip}}(x, r) = \sigma_{\text{dip}}(rQ_s(x)). \quad (3)$$

Indeed, the GBW model is used to describe the inclusive DIS data within a certain approximation. As is well known, this model is reasonable only at small transverse momenta k_t (after the Fourier transform), as its exponential decay contradicts the expected perturbative behavior at large k_t . The Bartels-Golec-Biernat-Kowalski (BGK) model [6], is another phenomenological approach to dipole cross section and reads

$$\sigma_{\text{dip}}(x, \mathbf{r}) = \sigma_0 \left\{ 1 - \exp \left(\frac{-\pi^2 r^2 \alpha_s(\mu^2) x g(x, \mu^2)}{N_c \sigma_0} \right) \right\}, \quad (4)$$

where $g(x, \mu^2)$ is the gluon collinear PDF. The dipole cross section in the BGK model is expanded into the DGLAP improved saturation model. In this paper we wish to evolve the dipole cross section directly into x and r using a Laplace transform technique and obtain an analytical method for the solution of the dipole cross section in terms of known initial gluon distribution. Then, we apply this analytical function to test the consistency of the saturation scale. We present unintegrated gluon distribution with and without Sudakov form factors from the evolution of the gluon density, which gives a good description of the gluon distribution owing to the parametrization methods.

2. Method

The color dipole cross section in the BGK model [6] reads

$$\sigma_{\text{dip}}(x, r) = \sigma_0 \left\{ 1 - \exp \left(-\frac{\sigma_{\text{DGLAP}}(x, r)}{\sigma_0} \right) \right\}, \quad (5)$$

*Electronic address: boroun@razi.ac.ir

where

$$\sigma_{\text{DGLAP}}(x, r) = \frac{\pi^2}{N_c} r^2 \alpha_s(\mu^2) x g(x, \mu^2), \quad (6)$$

with $N_c = 3$ [2, 7]. The hard scale, μ^2 , is assumed to be

$$\mu^2 = C/r^2 + \mu_0^2, \quad (7)$$

where the parameters C and μ_0^2 are obtained from the fit to the DIS data as summarized in [7]. The gluon distribution $xg(x, \mu^2)$ is dominant at low x in the DGLAP evolution equations [8–10] as the gluonic sector is

$$\frac{\partial G(x, \mu^2)}{\partial \ln \mu^2} \simeq \int_x^1 \frac{x}{y^2} dy P_{gg}\left(\frac{x}{y}, \alpha_s(\mu^2)\right) G(y, \mu^2), \quad (8)$$

where $G(x, \mu^2) = xg(x, \mu^2)$. The splitting function $P_{gg}(x, \alpha_s)$ at the higher-order corrections reads

$$P_{gg}(x, \alpha_s) = \frac{\alpha_s}{2\pi} P_{gg}^{\text{LO}}(x, \alpha_s) + \left(\frac{\alpha_s}{2\pi}\right)^2 P_{gg}^{\text{NLO}}(x, \alpha_s), \quad (9)$$

where the running coupling is defined by the following form in the leading-order (LO) renormalization group equation,

$$\mu^2 \frac{d\alpha_s(\mu^2)}{d\mu^2} = - \left(\frac{11C_A - 4T_R n_f}{12\pi} \right) \alpha_s^2(\mu^2) \quad (10)$$

with $C_A = N_c$, $T_R = \frac{1}{2}$ and $n_f = 4$ (the active quark flavor number).

Substituting Eq.(6) into (8), we can rewrite the evolution of $\sigma_{\text{DGLAP}}(x, r)$ as

$$\begin{aligned} \frac{\partial \sigma_{\text{DGLAP}}(x, \mu^2)}{\partial \ln \mu^2} &= -\alpha_s(\mu^2) r^2 \frac{\partial}{\partial \ln \mu^2} \left(\frac{1}{\alpha_s(\mu^2) r^2} \right) \times \\ &\sigma_{\text{DGLAP}}(x, \mu^2) + \int_x^1 \frac{x}{y^2} dy P_{gg}\left(\frac{x}{y}, \alpha_s(\mu^2)\right) \sigma_{\text{DGLAP}}(x, \mu^2). \end{aligned} \quad (11)$$

By writing

$$d \ln(\mu^2) = - \frac{2C}{r^3 \mu^2} dr, \quad (12)$$

we can rewrite Eq.(11) in the following form

$$\begin{aligned} d\sigma_{\text{DGLAP}}(x, r) &= \left[\frac{2}{r} + \frac{d \ln \alpha_s(r)}{dr} \right] dr \sigma_{\text{DGLAP}}(x, r) \\ &- \frac{2C}{r^3 \left(\frac{C}{r^2} + \mu_0^2 \right)} dr \int_x^1 \frac{x}{y^2} dy P_{gg}\left(\frac{x}{y}, \alpha_s(r)\right) \sigma_{\text{DGLAP}}(x, r). \end{aligned} \quad (13)$$

Now, we rewrite σ_{DGLAP} in Eq.(13) in terms of the variables $v = \ln(1/x)$ and r instead of x and r by using the notation $\hat{\sigma}_{\text{DGLAP}}(v, r) \equiv \sigma_{\text{DGLAP}}(e^{-v}, r)$ as

$$\begin{aligned} d\hat{\sigma}_{\text{DGLAP}}(v, r) &= \left[\frac{2}{r} + \frac{d \ln \alpha_s(r)}{dr} \right] dr \hat{\sigma}_{\text{DGLAP}}(v, r) \\ &- \frac{2C}{r^3 \left(\frac{C}{r^2} + \mu_0^2 \right)} dr \int_0^v \left[e^{-(v-w)} \hat{P}_{gg}(v-w, \alpha_s(r)) \right. \\ &\quad \left. \times \hat{\sigma}_{\text{DGLAP}}(w, r) \right] dw. \end{aligned} \quad (14)$$

In the following, we use the Laplace transform method developed in detail in [11–15] as $\mathcal{L}[\hat{\sigma}_{\text{DGLAP}}(v, r); s] \equiv \sigma_{\text{DGLAP}}(s, r)$ and using the fact that the Laplace transform of a convolution factors is simply the ordinary product of the Laplace transform of the factors, as

$$\begin{aligned} \mathcal{L} \left[\int_0^v \hat{\sigma}_{\text{DGLAP}}(w, r) \hat{H}(v-w, \alpha_s(r)) dw; s \right] \\ = \sigma_{\text{sD}}(s, r) \times h(s, \alpha_s(r)), \end{aligned} \quad (15)$$

where

$$\begin{aligned} h(s, \alpha_s(r)) &\equiv \mathcal{L}[e^{-v} \hat{P}_{gg}(v, \alpha_s(r)); s] = \frac{\alpha_s(r)}{2\pi} h^{(0)}(s) \\ &+ \left(\frac{\alpha_s(r)}{2\pi} \right)^2 h^{(1)}(s), \end{aligned} \quad (16)$$

where

$$\begin{aligned} h^{(0)}(s) &= \frac{33 - 2n_f}{6} + 6 \left(\frac{1}{s} - \frac{2}{1+s} + \frac{1}{s+2} \right. \\ &\quad \left. - \frac{1}{s+3} - \Psi(s+1) - \gamma_E \right), \end{aligned} \quad (17)$$

where $\Psi(x)$ is the digamma function and $\gamma_E = 0.5772156\dots$ is Euler's constant.

Therefore, we find

$$\begin{aligned} \sigma_{\text{sD}}(s, r) &= \sigma_{\text{sD}}(s, r_0) \left(\frac{r}{r_0} \right)^2 \frac{\alpha_s(r)}{\alpha_s(r_0)} \times \\ &\exp \left[- \frac{h^{(0)}(s)}{2\pi} \int_{r_0}^r \frac{2C\alpha_s(r)}{r^3 \left(\frac{C}{r^2} + \mu_0^2 \right)} dr \right. \\ &\quad \left. - \frac{h^{(1)}(s)}{(2\pi)^2} \int_{r_0}^r \frac{2C\alpha_s^2(r)}{r^3 \left(\frac{C}{r^2} + \mu_0^2 \right)} dr \right]. \end{aligned} \quad (18)$$

We keep the $1/s$ terms in the high-energy region of the coefficients $h^{(0)}(s)$ and $h^{(1)}(s)$ and apply the inverse Laplace transform as we find

$$\hat{\sigma}_{\text{DGLAP}}(v, r) \simeq \int_0^v \hat{\eta}(w, r, r_0) \hat{J}(v-w, \alpha_s(r)) dw, \quad (19)$$

where

$$\hat{\eta}(v, r, r_0) = \hat{\sigma}_{\text{DGLAP}}(v, r_0) \left(\frac{r}{r_0} \right)^2 \frac{\alpha_s(r)}{\alpha_s(r_0)}, \quad (20)$$

and

$$\hat{J}(v, \alpha_s(r)) = \delta(v) + \frac{\sqrt{-\xi}}{\sqrt{v}} \text{BesselI}(1, 2\sqrt{-\xi}\sqrt{v}), \quad (21)$$

where

$$\begin{aligned} \xi &= \frac{2C_A}{2\pi} \int_{r_0}^r \frac{2C\alpha_s(r)}{r^3 \left(\frac{C}{r^2} + \mu_0^2 \right)} dr \\ &+ \frac{(12C_F T_f - 46C_A T_f)}{9(2\pi)^2} \int_{r_0}^r \frac{2C\alpha_s^2(r)}{r^3 \left(\frac{C}{r^2} + \mu_0^2 \right)} dr, \end{aligned} \quad (22)$$

where $C_F = \frac{N_c^2 - 1}{2N_c}$ and $T_f = T_R n_f$.

Transforming back in to x space, $\sigma_{\text{DGLAP}}(x, r)$ is given by

$$\sigma_{\text{DGLAP}}(x, r) = \left(\frac{r}{r_0}\right)^2 \frac{\alpha_s(r)}{\alpha_s(r_0)} \left[\sigma_{\text{DGLAP}}(x, r_0) + \int_x^1 \sigma_{\text{DGLAP}}(z, r_0) \frac{\sqrt{-\xi}}{\sqrt{\ln \frac{z}{x}}} \text{BesselI}(1, 2\sqrt{-\xi} \sqrt{\ln \frac{z}{x}}) \frac{dz}{z} \right]. \quad (23)$$

Therefore, the evolution of the color dipole cross section is defined by the following form

$$\sigma_{\text{dip}}(x, r) = \sigma_0 \left\{ 1 - \exp\left(-\frac{1}{\sigma_0} \left(\frac{r}{r_0}\right)^2 \frac{\alpha_s(r)}{\alpha_s(r_0)} \left[\sigma_{\text{DGLAP}}(x, r_0) + \int_x^1 \sigma_{\text{DGLAP}}(z, r_0) \frac{\sqrt{-\xi}}{\sqrt{\ln \frac{z}{x}}} \text{BesselI}(1, 2\sqrt{-\xi} \sqrt{\ln \frac{z}{x}}) \frac{dz}{z} \right] \right) \right\}, \quad (24)$$

where

$$\sigma_{\text{DGLAP}}(x, r_0) = \frac{\pi^2}{N_c} r_0^2 \alpha_s(r_0) x g(x, r_0). \quad (25)$$

The initial gluon distribution at the scale μ_0^2 is defined in the form [2]

$$xg(x, \mu_0^2) = A_g x^{-\lambda_g} (1-x)^{C_g}, \quad (26)$$

where parameters are motivated by global fits to DIS data with respect to the results in Ref.[7].

Evolution of the gluon distribution with respect to the Laplace-transform method at low x is defined by

$$xg(x, \mu^2) \simeq xg(x, \mu_0^2) + \int_x^1 xg(z, \mu_0^2) \frac{\sqrt{\eta}}{\sqrt{\ln \frac{z}{x}}} \times \text{BesselI}(1, 2\sqrt{\eta} \sqrt{\ln \frac{z}{x}}) \frac{dz}{z}, \quad (27)$$

where

$$\eta = \int_{\mu_0^2}^{\mu^2} \left[\frac{3}{\pi} \alpha_s(\mu^2) - \frac{61}{9\pi^2} \alpha_s^2(\mu^2) \right] d\ln \mu^2. \quad (28)$$

The dipole cross section via a Fourier transform is related to the unintegrated gluon distribution (UGD) [1, 16] as the UGD¹, $f(x, k_t^2)$, is defined through the differential

integrated gluon distribution function by the following form

$$f(x, k_t^2) = \frac{\partial xg(x, \mu^2)}{\partial \ln \mu^2} \Big|_{\mu^2=k_t^2} \quad (29)$$

where the evolution of the UGD is find

$$f(x, k_t^2) = \int_x^1 xg(z, \mu_0^2) \frac{\partial}{\partial \ln \mu^2} \left[\frac{\sqrt{\eta}}{\sqrt{\ln \frac{z}{x}}} \times \text{BesselI}(1, 2\sqrt{\eta} \sqrt{\ln \frac{z}{x}}) \frac{dz}{z} \right] \Big|_{\mu^2=k_t^2} \quad (30)$$

Unintegrated distribution is modified by the Sudakov form factor [30, 31] so that the UGD remains true as x increases or decreases [32, 33]. We find

$$f^S(x, k_t^2) = \left[xg(x, \mu_0^2) \frac{\partial}{\partial \ln \mu^2} e^{-S(r, \mu^2)} + \int_x^1 xg(z, \mu_0^2) \frac{\partial}{\partial \ln \mu^2} \left[e^{-S(r, \mu^2)} \frac{\sqrt{\eta}}{\sqrt{\ln \frac{z}{x}}} \times \text{BesselI}(1, 2\sqrt{\eta} \sqrt{\ln \frac{z}{x}}) \frac{dz}{z} \right] \right] \Big|_{\mu^2=k_t^2} \quad (31)$$

with

$$S_{\text{pert}}(r, \mu^2) = \frac{C_A}{2\pi b_0} \left[-\ln \left(\frac{\mu^2}{\mu_b^2} \right) + \left(\frac{1 + \alpha_s(\mu_b^2) b_0 \ln \left(\frac{\mu^2}{\mu_b^2} \right)}{\alpha_s(\mu_b^2) b_0} \right) \times \ln \left(1 + \alpha_s(\mu_b^2) b_0 \ln \left(\frac{\mu^2}{\mu_b^2} \right) \right) \right], \quad (32)$$

where $\mu_b = 2e^{-\gamma_E}/r$ and $\gamma_E \approx 0.577$ is the Euler-Mascheroni constant.

3. Results

In Fig.1, using the initial scale for the gluon distribution $xg(x, \mu_0^2)$ in Eq.(26) and Table I, we have plotted the gluon distribution function, $xg(x, \mu^2)$, from Eq.(27) as a function of x (for $x < 0.1$) for the values of $\mu^2 = 1.9, 10$ and 100 GeV^2 at the leading-order (LO) approximation and compared with the CJ15 parametrization method [34] as accompanied by the total errors. The gluon distribution extracted at μ^2 values are in good agreement with the CJ15 data. The QCD parameter Λ for four numbers of active flavor has been extracted due to $\alpha_s(M_z^2) = 0.1166$ in comparison with the CJ15 results with $\alpha_s(M_z^2) = 0.136668$.

In Fig. 2 we show the logarithmic k_t^2 -derivative of the evolution of gluon distribution as a function of k_t^2 for three values of x . We observe that the function $f(x, k_t^2)$ increases as k_t^2 increases and the variable x decreases. The behavior of UGD decreases as k_t^2 decreases to

¹ The different models [4, 17–21] have been derived where relative the UGD to the k_t factorization and have been compared in Refs.[22–28] as:

- In the IN model [17] a UGD soft-hard model has been proposed in the large- and small- k_t region.
- The ABIPSW model [18] is a x -independent UGD model.
- The HSS model [19] is defined to take a convolution form between the BFKL gluon Green's function and the leading-order of the proton impact factor.
- The WMR model [20] gives the probability of evolving from the scale k_t on an extra-scale μ at fixed Q .
- The GBW model [4, 21] is derived from the dipole cross section.
- The UGD model based on gluon TMDs is considered in Refs.[27, 29].

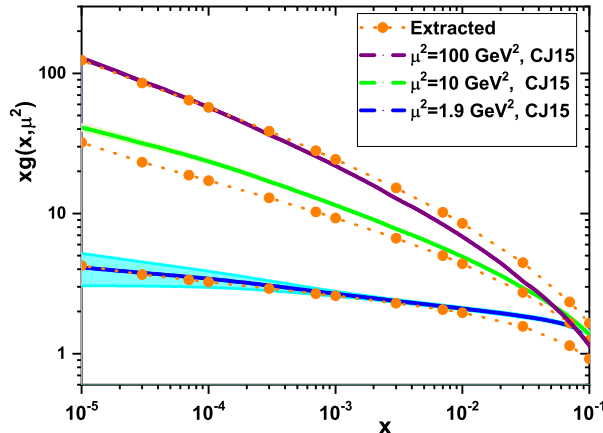


FIG. 1: The extracted $xg(x, \mu^2)$ as a function of x compared with the CJ15LO parametrization method [34] at $\mu^2 = 1.9, 10$ and 100 GeV^2 .

TABLE I: The fixed parameters of the gluon density at the initial scale and dipole cross section according to Ref.[7] with $m_c = 1.4 \text{ GeV}$.

| $\mu_0^2 [\text{GeV}^2]$ | C | $\sigma_0 [\text{mb}]$ | A_g | λ_g | C_g |
|--------------------------|------|------------------------|-------|-------------|-------|
| 1.73 | 0.38 | 22.40 | 1.35 | 0.079 | 5.6 |

$k_t^2 < 1 \text{ GeV}^2$. The resulting UGD with the k_t^2 dependence from the evolution of the gluon distribution and comparison with the HSS [19], IN [19] and WMR [20] models at $x = 10^{-3}$ and $x = 10^{-4}$ are shown in Figs.3 and 4 respectively. We observe that the results in Figs.3 and 4, due to the evolution of the gluon distribution, are comparable to the models (especially IN-CT14 LO) at moderate k_t^2 . The behavior of the UGD at small and large k_t^2 in Figs.3 and 4 decreases and increases in comparison with the models respectively. There is an improved model (i.e., Eq.(31)) due to the Sudakov form factor, which increases and decreases the UGD behavior at small and large values of k_t^2 respectively. In Fig.5, we show the effects of this correction in the ratio $R_f = \frac{f^S(x, k_t^2)}{f(x, k_t^2)}$ for $k_t^2 \geq 2 \text{ GeV}^2$.

We have calculated the r dependence of the ratio $\sigma_{\text{dip}}/\sigma_0$ for $x = 10^{-5}$ and 10^{-3} at the LO and NLO approximations² from the evolution of the dipole cross section, Eq.(24), and compared with the GBW model, Eq.(2), in Fig.6. The evolution of the dipole cross section gives a similar description of the ratio $\sigma_{\text{dip}}/\sigma_0$ in comparison with the GBW model at low x . The

² The charm quark mass is taken to account in this analysis.

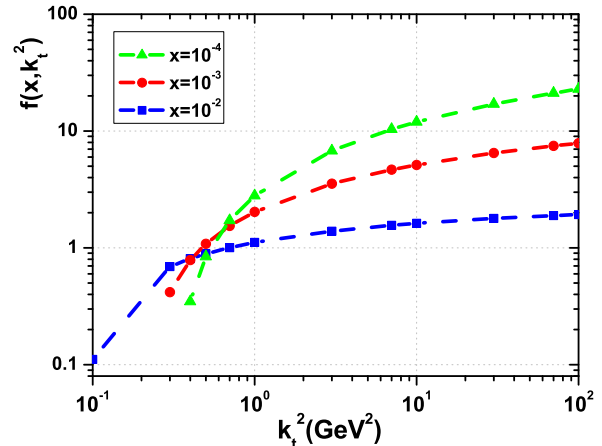


FIG. 2: The evolution of the unintegrated gluon distribution from Eq.(30).

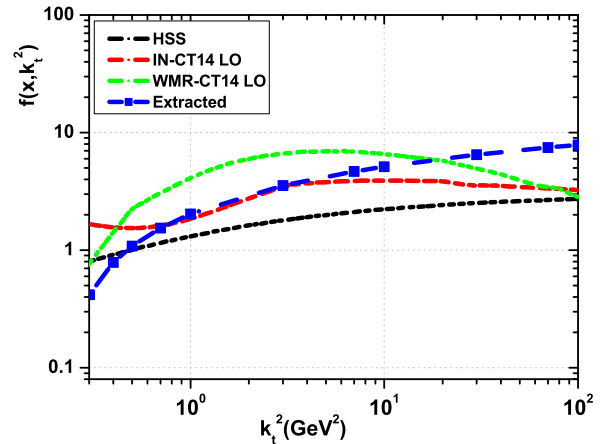


FIG. 3: UGD extracted (square-dash curve) from the evolution of gluon distribution compared with Hentschinski et al. [19], Ivanov and Nikolaev [17], and Watt et al. [20] models (dashed curves) as a function of k_t^2 at $x = 10^{-3}$.

transition point between the large and small r regimes³ in the evolution model (i.e., Eq.(24)) increases to the lower r values in comparison with the GBW model, although is governed by the increasing with x saturation radius $R_0(x) \equiv \frac{1}{Q_s(x)}$. The evolution model is guaranteed that the dipole cross section saturates for smaller dipole

³ At small r , σ_{dip} features colour transparency which is pQCD phenomenon and for large r it saturates [4].

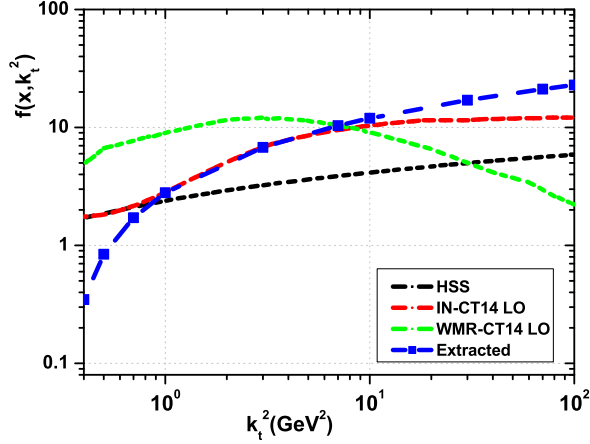


FIG. 4: The same as Fig.3 for $x = 10^{-4}$.

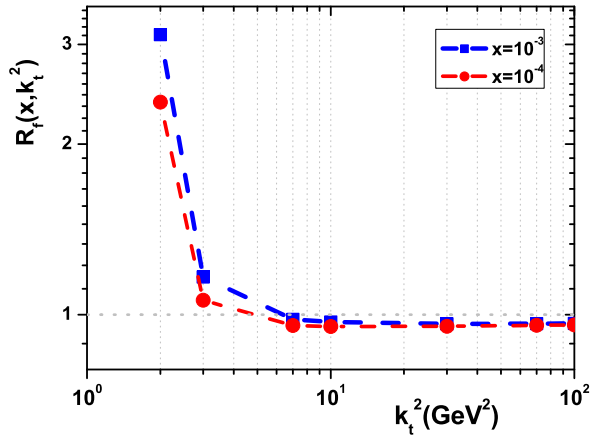


FIG. 5: The ratio of Sudakov form factor effect in the UGD for $x = 10^{-3}$ and $x = 10^{-4}$ at $k_t^2 \geq 2 \text{ GeV}^2$.

size in comparison with the GBW model and decreasing x .

The evolution of the dipole cross section (i.e., Eq.(24)) has a property of geometric scaling as it becomes a function of a single variable, rQ_s , for all values of r and x . In Fig.7, we show the ratio $\sigma_{\text{dip}}(rQ_s(x))/\sigma_0$ in the evolution method in the single variable $rQ_s(x)$ for all values of x and r at the LO and NLO approximations. The results at $x = 10^{-5}$ and 10^{-3} merge into one solid line where this is a reflecting of geometrical scaling. This geometrical scaling is visible in the region $rQ_s(x) \geq 0.2$ together with its violation for $rQ_s(x) < 0.2$ in comparison with the GBW model.

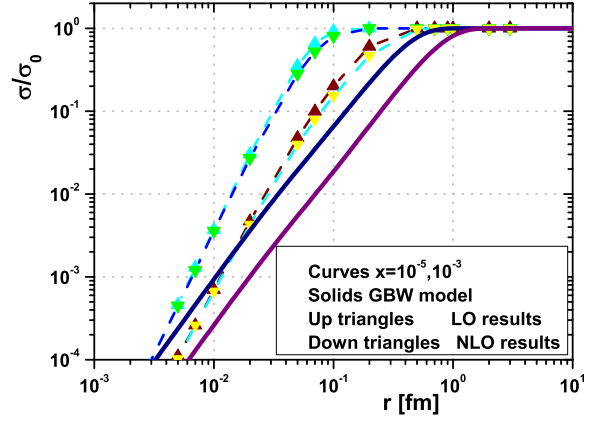


FIG. 6: The extracted ratio $\sigma_{\text{dip}}/\sigma_0$ as a function of r for $x = 10^{-5}$ and 10^{-3} (curves from left to right, respectively) at the LO (up triangles) and NLO (down triangles) approximations from the evolution of the dipole cross section, Eq.(24), compared with the GBW model (solid curves), Eq.(2).

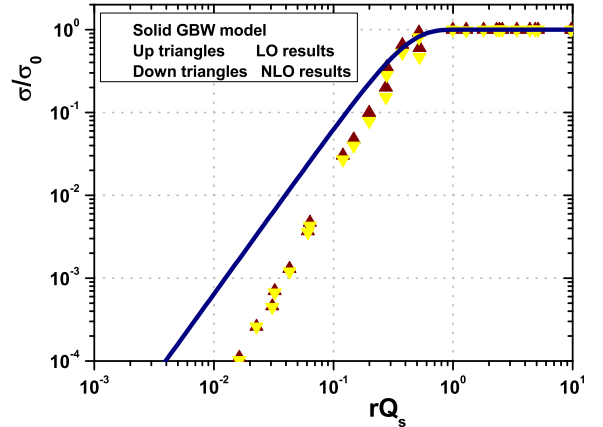


FIG. 7: The extracted ratio $\sigma_{\text{dip}}(rQ_s(x))/\sigma_0$ as a function of $rQ_s(x)$ at the LO (up triangles) and NLO (down triangles) approximations from the evolution of the dipole cross section, merges into one line due to the geometric scaling compared with the GBW model (solid curve).

In conclusion, we have presented a method based on the Laplace transform method to determine the evolution of the dipole cross section at the LO and NLO approximations. This method relies on the BGK method within a kinematical region characterized by low values of the Bjorken variable x in a wide range of transverse size r . In the first part of this analysis, we obtained a new evolution for the integrated and

unintegrated gluon distributions in a wide range of μ^2 and k_t^2 respectively. We have shown that the evolution of integrated gluon distribution is comparable with the CJ15 parametrization group in a wide range of μ^2 and x and also the evolution of unintegrated gluon distribution is comparable with the UGD models in a wide range of k_t^2 . The effects of the Sudakov form factor were investigated for the UGD in a wide range of k_t^2 . The effect is visible with a small and large value of k_t^2 . In the second part of our study, we have compared the evolution of the color dipole cross section with the GBW model in a wide range of r at low values of x . This evolution method allows to extend the GBW saturation model to low values of dipole size r (or large values of Q^2) and shows that the saturation scale and geometric scaling are retained in the region $rQ_s(x) \geq 0.2$.

ACKNOWLEDGMENTS

The author is thankful to Razi university for financial support of this project and would like to thank Professor Jen-Chieh Peng and B. Z. Kopeliovich for useful comments.

-
- [1] N. N. Nikolaev and B. G. Zakharov, Phys. Lett. B **332**, 184 (1994).
- [2] A. Luszczak, M. Luszczak and W. Schäfer, Phys.Lett.B **835**, 137582 (2022).
- [3] J. T. Amaral, D. A. Fagundes and M. V. T. Machado, Phys. Rev. D **103**, 016013 (2021); J. Raufeisen and J.-C. Peng, Phys.Rev.D **67**, 054008 (2003); Yu S.Jeong, C.S.Kim and M. Vu Luu, JHEP **11**, 025 (2014); B. Z. Kopeliovich, I. K. Potashnikova, Ivan Schmidt, Phys.Rev.C **81**, 035204 (2010).
- [4] K.Golec-Biernat, Acta.Phys.Polon.B **33**, 2771 (2002); Acta.Phys.Polon.B **35**, 3103 (2004); J.Phys.G **28**, 1057 (2002).
- [5] A. M. Stasto, K. J. Golec-Biernat and J. Kwiecinski, Phys. Rev. Lett. **86**, 596 (2001).
- [6] J.Bartels, K.Golec-Biernat and H.Kowalski, Phys. Rev. D **66**, 014001 (2002).
- [7] K. Golec-Biernat and S.Sapeta, JHEP **03**, 102 (2018).
- [8] . Yu.L.Dokshitzer, Sov.Phys.JETP **46**, 641 (1977).
- [9] G.Altarelli and G.Parisi, Nucl.Phys.B **126**, 298 (1977).
- [10] V.N.Gribov and L.N.Lipatov, Sov.J.Nucl.Phys. **15**, 438 (1972).
- [11] Martin M. Block, Loyal Durand, and Douglas W. McKay, Phys. Rev. D **79**, 014031 (2009).
- [12] Martin M. Block, Loyal Durand, Phuoc Ha, and Douglas W. McKay, Phys. Rev. D **83**, 054009 (2011).
- [13] Martin M. Block, Loyal Durand, Phuoc Ha, and Douglas W. McKay, Phys. Rev. D **84**, 094010 (2011).
- [14] Martin M. Block, Loyal Durand, Phuoc Ha, and Douglas W. McKay, Phys. Rev. D **88**, 014006 (2013).
- [15] G.R.Boroun and Phuoc Ha, Phys. Rev. D **109**, 094037 (2024).
- [16] N. N. Nikolaev and W. Schäfer, Phys. Rev. D **74**, 014023 (2006).
- [17] I.P.Ivanov and N.N.Nikolaev, Phys.Rev.D **65**, 054004 (2002).
- [18] I.V. Anikin, A. Besse, D.Yu. Ivanov, B. Pire, L. Szymanowski and S. Wallon, Phys. Rev. D **84**, 054004 (2011).
- [19] M. Hentschinski, A. Sabio Vera and C. Salas, Phys. Rev. Lett. **110**, 041601 (2013).
- [20] G. Watt, A.D. Martin and M.G. Ryskin, Eur. Phys. J. C **31**, 73 (2003).
- [21] K.Golec-Biernat and M.Wüsthoff, Phys. Rev. D **59**, 014017 (1998).
- [22] A.D.Bolognino, F.G.Celiberto, Dmitry Yu. Ivanov and A.Papa, Frascati Phys.Ser. **67**, 76 (2018).
- [23] A.D.Bolognino, F.G.Celiberto, Acta Phys.Polon.Supp. **12**, 891 (2019); Eur.Phys.J.C **78**, 1023 (2018).
- [24] F.G.Celiberto, Nuovo Cim. C **42**, 220 (2019); Eur.Phys.J.C **84**, 384 (2024).
- [25] F.G.Celiberto, D. Gordo Gomez and A.Sabio Vera, Phys.Lett.B **786**, 201 (2018).
- [26] A.D.Bolognino, A.Szczurek and W. Schäfer, Phys.Rev.D **101**, 054041 (2020).
- [27] A.D.Bolognino, F.G.Celiberto, D.Y.Ivanov, A.Papa, W.Schäfer and A.Szczurek, Eur.Phys.J.C **81**, 846 (2021); A. Bacchetta, F.G. Celiberto, M. Radici, P. Taels, Eur. Phys. J. C **80**, 733 (2020).
- [28] G.R.Boroun, Eur.Phys.J.C **83**, 42 (2023); Eur.Phys.J.C **82**, 740 (2022); Phys.Rev.D **108**, 034025 (2023); Eur.Phys.J.A **60**, 48 (2024).
- [29] A. V. Lipatov , G.I. Lykasov and M.A. Malyshev, arXiv [hep-ph]:2301.09967; A.V.Kotikov, A.V.Lipatov and P.M.Zhang, Phys.Rev.D **104**, 054042 (2021).
- [30] M. A. Kimber, A. D. Martin and M. G. Ryskin, Eur. Phys. J. C **12**, 655 (2000).
- [31] B.W. Xiao, F. Yuan and J. Zhou, Nucl. Phys. B **921**, 104 (2017).
- [32] M. A. Kimber, J. Kwiecinski, A. D. Martin, and A. M. Stasto, Phys. Rev. D **62**, 094006 (2000).
- [33] T. Goda, K. Kutak and S. Sapeta, Eur.Phys.J.C **83**, 957 (2023).
- [34] J. F. Owens, A. Accardi and W. Melnitchouk, Phys.Rev.D **87**, 094012 (2013).